

An Image-Based Approach for Loamy Soil Dryness Classification Using SVM and Hybrid Features

S M Abdullah Al Shuaeb^{a*}, Md. Mizanur Rahman^b, Mahbubun Nahar^c, Utpal Kanti Roy^d, Al Fahad^e

^a*Bangladesh Agricultural University, Mymensingh, Bangladesh*

^{b,c}*Dept. of Computer Science and Engineering, Jatiya Kabi Kazi Nazrul Islam University, Bangladesh*

^d*Dept. of Computer Science and Engineering, City University Bangladesh*

^e*Department of Civil Engineering, Jeonbuk National University, South Korea*

^a*Email:nixon.cse28@gmail.com*

^c*Email:mahbuba.knu@gmail.com*

Abstract

Correctly identifying the moisture and dryness of loamy soil is essential to maintain agricultural productivity. Since loamy soil is favorable for crop root growth, its physical and moisture properties play an important role in determining irrigation management, crop planning, and soil development strategies. In conventional methods, soil moisture and dryness are usually determined by cutting or lifting samples from the soil and transporting them to the laboratory, which directly interferes with the natural structure and condition of the soil. Such methods are considered invasive, time-consuming, and relatively expensive. In order to overcome these limitations, in this study, we proposed a fast, non-invasive, and image-based method for predicting the dryness level of loamy soil, where hybrid image features and a support vector machine (SVM) classifier are used. In the proposed method, a comprehensive feature vector is formed by adding color features, Local Binary Pattern (LBP), Haralick texture features, and Histogram of Oriented Gradients (HOG) features extracts from soil images. Subsequently, different SVM models with linear, Radial Basis Function (RBF), and polynomial kernels were trained and evaluated using these feature vectors to classify the dryness of loamy soil into five categories: very dry, dry, moist, wet, and very wet. Experimental results indicate that the proposed model achieved high accuracy, precision, recall, and F1-score, which proves the effectiveness of the hybrid features and SVM kernels used, the stability of the model, and its applicability in real situations. Overall, the proposed image-based non-invasive method can be considered as a fast, cost-effective, and practical alternative for assessing the dryness of loamy soil by reducing the reliance on conventional laboratory-based techniques.

Keywords: Haralick feature; HOG feature; Support Vector Machine (SVM); Machine Learning (ML).

Received: 11/16/2025

Accepted: 1/16/2026

Published: 1/26/2026

* Corresponding author.

1. Introduction

Soil moisture is an essential element for a healthy and sustainable agricultural system. It directly affects plant growth, crop production, and the overall functioning of the land ecosystem. Loamy soil is one of the most suitable soils for agriculture, as it contains a nearly equal mixture of sand, silt, and clay. This balanced composition is capable of retaining sufficient water while also allowing excess water to drain away, creating a favourable environment for a variety of crops. However, changes in the moisture level of loamy soil can significantly affect its fertility and plant growth. If the soil becomes too dry or too wet, crop production can decrease, irrigation water wastage can increase, and overall agricultural productivity can decrease. Therefore, determining the dryness of loamy soil and selecting suitable soil is a very important step before planting crops.

Several methods are used to determine soil properties, among which chemical testing and image analysis are widely applied. Chemical tests are usually carried out in laboratories using various chemicals, which are expensive, time-consuming, and not easily accessible to most farmers. On the other hand, image analysis-based methods use soil colour and texture as key indicators to determine the dryness status. Soil colour and appearance are indicative of many physical and chemical properties, although they may vary due to environmental changes, location, or natural processes.

Recent studies have attempted to classify soil moisture using image analysis, showing promise as a fast, cost-effective, and non-invasive alternative to traditional methods[1,2] . Acharjee and his colleagues[3] offered a machine learning model to predict crop yield and soil moisture. On the other hand, RGB image processing has been used for iron and carbon prediction from soil images. The moisture content of the soil was classified using the CIEL*a*b* mode, and the depth of soil was estimated by L*a*b* mode [4]. The scheme of [5] offered soil water content accuracy in sandy Loamy soil. Asensio and his colleagues [6]

developed model to forecast eighteen soil characteristics, including carbon, nitrogen, iron, sand, and clay, using RGB image processing. Another soil texture image classification as offered by [7]. RGB histogram analysis was used to classify the soil surface image in this study. Jiao and his colleagues [8] offered a chip less soil moisture sensor device called SoilTAG, which uses battery-free inactive tags to determine soil moisture levels. Moreover, Liu and his colleagues [9] developed an analysis approach based on support vector machines (SVM) to identify the urban soil. Machbah and his colleagues [10] offered a novel features-based machine learning model to classify the soil type. This study shows that image processing-based techniques are gradually gaining popularity in predicting the moisture level of loamy soil due to their shorter time to results and relatively low cost compared to conventional chemical methods. However, to our knowledge, most of the existing studies still lack sufficient accuracy and stability. In this context, we have prepared our own image-based dataset of loamy soil and proposed a hybrid feature-based method for predicting the dryness level of loamy soil by training an SVM model with various kernel functions (such as linear, RBF, and polynomial) using rich hybrid image features. Experimental results show that the proposed method achieves more promising accuracy than previous works. As a result, this method can make significant contributions to improving irrigation management, making soil selection more information-based, and ultimately increasing crop yields by more accurately predicting the moisture status of loamy soil.

The main contribution of this paper are:

1. We have collected loamy soil images with different moisture levels.
2. The image dataset will be made public and available for use by other researchers.
3. We have created an SVM with different kernel functions for predicting loamy soil dryness levels.
4. Due to limited studies on loamy soil moisture, we analyzed it and found that our model outperforms existing studies across key metrics features extraction, classifying the dryness.

This work is organized as follows. We offer the details “Introduction” to detect Loamy dryness soil levels in Section 1. “Proposed methodology” In Section 2. Experiment and result.

2. Methodology

As shown in Figure 1, the proposed method relies on image analysis to predict the dryness level of loamy soil. The workflow consists of five key stages: image acquisition, image preprocessing, feature extraction, dryness classification, and performance evaluation.

Image Acquisition: Loamy soil samples were collected from several croplands in the Jamuna River watershed of Tangail district, Bangladesh. More detailed information about the dataset will be supplied in the result section.

Image Preprocessing: The performance of the model may be impacted by the many kinds of noise present in images taken in a laboratory setting. Furthermore, high-resolution images taken with iPhones have very large sizes, so necessitating more processing. To address the issues, following the image processing steps were applied as shown in Figure 2(a)–(e).

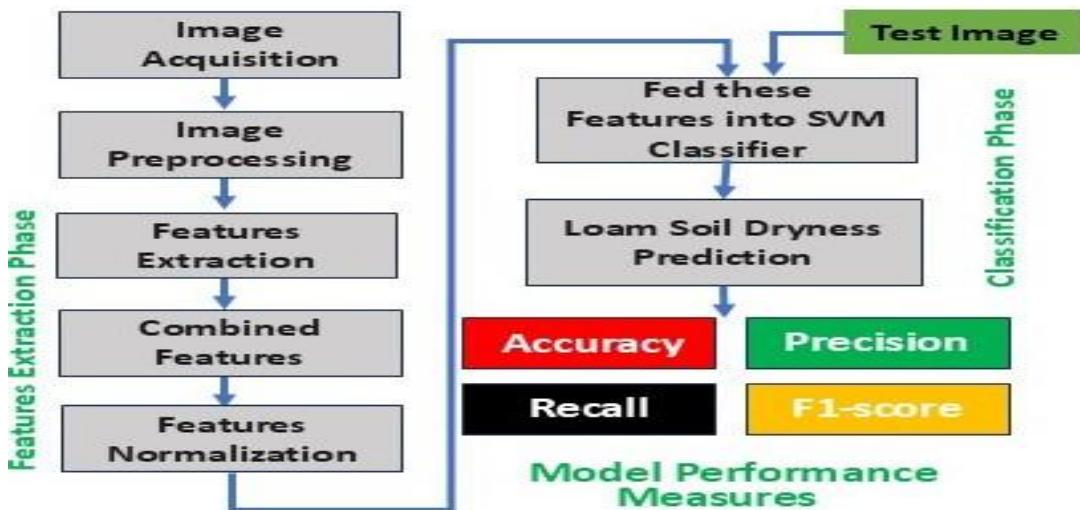


Figure1: Proposed Methodology

Resizing: To ensure that every picture is the same size and appropriate for model input, each one was scaled to 250 by 250 pixels.

Colour Conversion: RGB colour images were converted to grayscale, which may help eliminate extraneous details when extracting features.

Noise reduction: To enhance picture quality, the median filter was used, which effectively lowers speckle and lobe noise [11,12].

Contrast Enhancement: To increase the distribution of pixel values and make picture details more visible, histogram equalization was used. These preprocessing steps convert the images into high-quality, model-ready inputs [13,14].

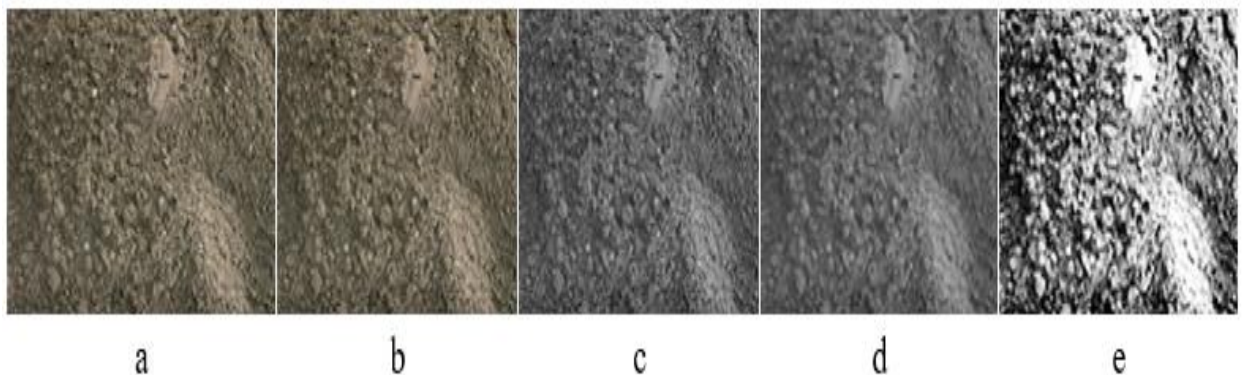


Figure 2: Sequential display of the original RGB (a), resized to 250×250 (b), converted to grayscale (c), denoised using median filtering (d), and contrast-enhanced via histogram equalization (e) images

Feature Extraction Phase: Feature extraction is the process of obtaining valuable information from an image. Images of Loamy soil were analysed using feature extraction techniques in our suggested system [15,16]. Our suggested method calculated the moisture content of Loamy soil by extracting colour, LBP (Local Binary Pattern), Haralick texture, and Histogram of Oriented Gradients (HOG) features from soil images. The colour feature calculates the colour variation of the soil by analysing the average value of the RGB (red, green, blue) channels of the image. Dry soil generally appears light; while wet soil is dark this colour variance is clearly shown in the RGB value. As a result, the RGB based colour feature helps the classifiers to softly difference the dryness or wetness of the soil. Moreover, Local Binary Pattern explores the pattern around each pixel in the image to generate a binary code. LBP also provides vital information about the texture of the soil. By extracting these texture features in the form of histogram, the svm classifier can easily distinguish various soil dryness levels. Furthermore, Haralick characteristics are produced from the Gray Level Co-occurrence Matrix (GLCM), which records the spatial correlations between pixel intensities and provides useful texture data[4,7,10,17,18,19]. These features are retrieved and concatenated into a single feature vector, which is then normalized using Min-Max Normalization. An SVM model trained on this normalized feature vector is able to predict the moisture content of Loamy soil. Haralick features are calculated from the Gray Level Co-Occurrence Matrix (GLCM). Let, an image $I(x, y)$, the GLCM $P(i, j)$ is computed as:

$$P(i, j) = \sum_{x=1}^M \sum_{y=1}^N \begin{cases} 1, & \text{if } I(x, y) = i \text{ and } I(x + \Delta x, y + \Delta y) = j \\ 0, & \text{otherwise} \end{cases} \quad \text{Equation (1)}$$

Where i, j are pixel intensities and $(\Delta x, \Delta y)$ defines the spatial offsets.

Typical Haralick characteristics taken from GLCM:

Contrast: Measures the intensity variation.

$$\sum_{i,j} P(i,j) (i - j)^2 \quad \text{Equation (2)}$$

Correlation: Measures how correlated pixels are:

$$\sum_{i,j} \frac{(i - \mu_i)(j - \mu_j)P(i,j)}{\sigma_i \sigma_j} \quad \text{Equation (3)}$$

Energy: Measures uniformity:

$$\sum_{i,j} P(i,j)^2 \quad \text{Equation (4)}$$

Homogeneity: Measures closeness of pixel pairs:

$$\sum_{i,j} \frac{P(i,j)}{1 + |i - j|} \quad \text{Equation (5)}$$

Histogram of Oriented Gradients (HOG): HOG is a feature descriptor that records an image's gradient intensity and edge directions. It is very helpful for recognizing patterns and textures. Mathematical function of HOG is Compute the gradient G_x and G_y using Sobel filters. Where $G_x = I * S_x$, $G_y = I * S_y$ Eq (6). Where S_x and S_y are Sobel operators. Compute gradient magnitude and orientation.

Mathematically,

$$M = \sqrt{G_x^2 + G_y^2} \quad \text{Equation (7)}$$

$$\theta = \tan^{-1} \frac{G_y}{G_x} \quad \text{Equation (8)}$$

We created a single feature vector by combining the Colour, LBP, Haralick and HOG features after they were extracted. Mathematically,

$$FV = Color + Lbp + Haralick + HOG \quad \text{Equation (9)}$$

To ensure that all features are equally scaled, we applied Min-Max Normalization. Mathematically,

$$F_{norm} = \frac{F - F_{min}}{F_{max} - F_{min}} \quad \text{Equation (10)}$$

Classification Phase: Support Vector Machine (SVM) is a supervised learning algorithm that works by finding

an optimal hyperplane that separates data points of classes. In this study, multiclass SVM model was utilized to classify Loamy soil images into five dryness categories: Very Dry, Dry, Moisture, Wet, and Very Wet. After extracting colours, Ibp, Haralick, and HOG features, all feature vectors are normalized using Min-Max normalization so that no feature dominates due to scale. These normalized features act as input for the SVM classifier with different kernel functions namely linear, rbf, and polynomial respectively. The SVM aims to find an optimal hyperplane $w^T x + b = 0$ that separates the feature space into different dryness classes. The decision function is given as:

$$f(x) = \text{sign}(w^T x + b) \quad \text{Equation (11)}$$

Here, x is the input feature vector, w is the weight vector, and b is the bias term. The SVM selects support vectors (important training data points) that lie closest to the hyperplane. It maximizes the margin between the hyperplane and the support vectors to ensure better generalization. This optimization is given by:

$$\min_{w,b} \frac{1}{2} \|w\|^2 \text{ subject to } y_i(w^T x_i + b) \geq 1 \quad \text{Equation (12)}$$

Since this problem involves 5 classes (multi-class), we used a One-vs-One (OvO) strategy, where multiple binary SVM classifiers are trained, and their results are aggregated to decide the final class[20,21,22,23,24,25,26,27]. During testing, the input image undergoes the same feature extraction and normalization process. The trained SVM model then predicts the class label using the decision function. The predicted class is compared with the actual label, and performance is measured using standard evaluation metrics like Accuracy, Precision, Recall, and F1-Score. Following the classification process, the computer makes a prediction regarding the dryness categories of the Loamy soil, namely (dry, very dry, moisture, wet, and very wet) images.

Model Performance Evaluation: The performance of the model is evaluated using four standard metrics. This step makes sure that the model can correctly classify the levels of dryness in Loamy soil using image-based analysis so that the soil condition rating can go more smoothly[28,29,30,31]. The four standard metrics are discussed here respectively.

Accuracy: Overall correctness of predictions. Mathematically,

$$\text{Accuracy} = \frac{TP+TN}{TP+TN+FP+FN} \quad \text{Equation (13)}$$

where TP, TN, FP and FN represent the true positive, true negative, false positive, and false negative respectively.

Precision: Correct positive predictions. Mathematically,

$$\text{Precision} = \frac{TP}{TP+FP} \quad \text{Equation (14)}$$

Recall: Ability to detect all positives. Mathematically,

$$Recall = \frac{TP}{TP+FN} \quad Equation (15)$$

F1-score: Balance of precision & recall. Mathematically,

$$F - Score = \frac{2*(recall*precision)}{recall+precision} \quad Equation (16)$$

3. Experiment and Result Analysis

This section discusses the preparation of datasets and the performance of the proposed SVM machine learning model with various kernels functions like linear, RBF, and polynomial respectively. This section also discusses Loamy soil dryness levels prediction accuracy, precision, recall, and f1-score with different features settings, precision-recall curve, RGB Intensity Distributions of Different Loamy Soils, features importance, and comparison with recent study respectively.

Dataset Collection and Representation: We discussed it earlier in the image acquisition section Soil samples were collected from many croplands in the Jamuna River region of Tangail district, Bangladesh. Following collection, the soil was imaged in a controlled environment. An iPhone11 was used to ensure accurate and high-quality images. Each shot was taken from a certain distance, i.e. 60.96 cm. This procedure was used continually to ensure that the image quality was maintained and suitable for analysis.

Table 1: demonstrate the augmentation techniques applied to the Loamy soil dataset

S	Loamy	Soil	Original	Rotation	Scaling	Reflection	(Total Original + Augmentation
N	Dryness		Image	(angles 90 to 180)	(up- down)	(Horizontal- Vertical)	Image)
1	Dry		150	2×150	2×150	2×150	1050
2	Very Dry,		150	2×150	2×150	2×150	1050
3	Moisture,		150	2×150	2×150	2×150	1050
4	Very Wet		150	2×150	2×150	2×150	1050
5	Wet		150	2×150	2×150	2×150	1050
The dataset contains the total number of Loamy soil images							5,250

Table 1 demonstrates the final image augmentation techniques applied to initial the Loamy soil dataset. Initially, 150 original images were gathered for each Loamy soil class. Subsequently, various augmentation techniques were used to increase the size of the dataset and improve the generalization ability of the suggested method. First, each image was rotated by two angles (90° and 180°) using rotation, which resulted in 300 additional images from each category. Then, each image was downscaled and upscaled once using Scaling, which resulted in 300 new images. In addition, each image was reflected once horizontally and once vertically applying Reflection, which resulted in 300 additional images for each category. As a result of these augmentations, 900

additional images were added to the 150 original images in each class, for a total of 1050 images. Since the study used five Loamy soil categories (very dry, dry, moisture, wet, and very wet), the total size of the entire dataset is 5250 images. Initially, the dataset had only 750 images, but through the augmentation process, it was increased to 5,250. These augmentation techniques not only expanded the size of the dataset, but also enhanced the diversity of the Loamy soil images, which is essential for increasing the performance and reliability of the model.

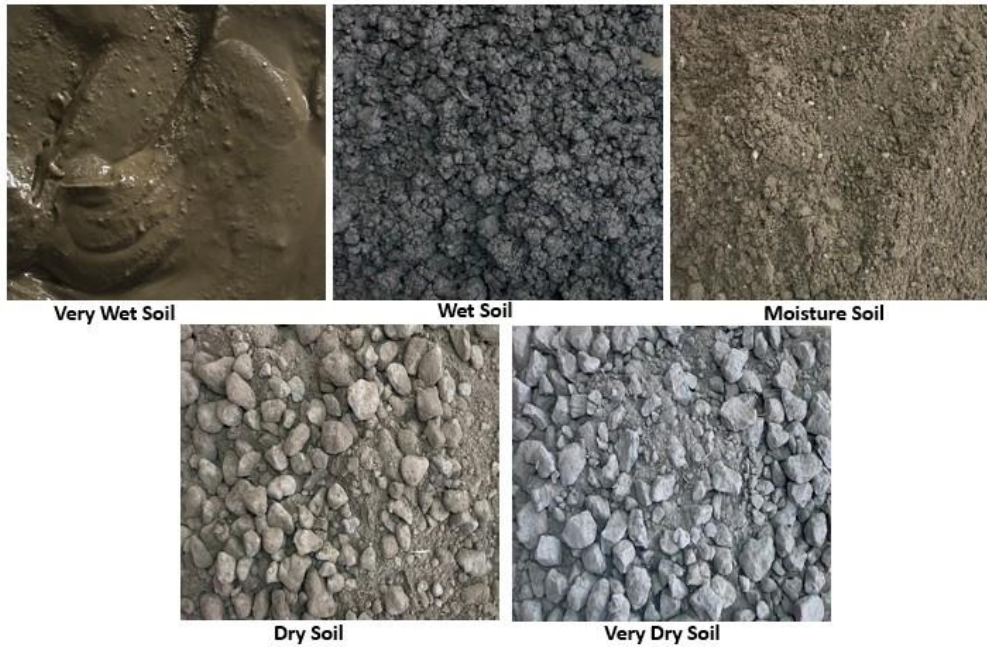


Figure 3: Five different classes of Loamy soil samples

Hence, Table 1 describes the summary of the prepared dataset and the dataset snippet are shown in Figure 3.

Explanation of Different Experimental Settings: The performance results for the proposed loam soil dryness classification method in table 2 are presented using different feature sets and three types of SVM kernel functions (linear, RBF, and polynomial). A 10-fold iterative $10 \times (80/20)$ cross-validation method was used to evaluate the performance, where 80% of the base image is used for training and the remaining 20% is used for testing. During model development, augmentation is applied only on the training set, where rotation (90° and 180°), scaling (0.8 and 1.2 times), and horizontal and vertical flipping (horizontal and vertical reflection) are used for the image. On the other hand, only the original (non-augmented) base image is used for testing, making the evaluation process more realistic and unbiased. The main performance metrics for the sample model are accuracy, precision, recall, and F1-score.

Table 2: Performance scores for different feature sets on the augmented image dataset

Feature Set	SVM Kernel Function	Accuracy	Precision	Recall	F1-score
Only color	Linear	0.89067	0.90738	0.89067	0.89158
	RBF	0.94133	0.94101	0.94133	0.94103
	Polynomial	0.96133	0.96196	0.96133	0.96154
Only Haralick	Linear	0.91333	0.91438	0.91333	0.91007
	RBF	0.94800	0.94779	0.94800	0.94774
	Polynomial	0.96133	0.96145	0.96133	0.96134
Only HOG	Linear	0.39733	0.29916	0.39733	0.33083
	RBF	0.40267	0.45017	0.40267	0.28548
	Polynomial	0.39467	0.37916	0.39467	0.32157
Only LBP	Linear	0.98400	0.98400	0.98400	0.98400
	RBF	0.99467	0.99470	0.99467	0.99467
	Polynomial	0.99733	0.99737	0.99733	0.99733
Color + Haralick	Linear	0.97867	0.98072	0.97867	0.97861
	RBF	0.99467	0.99467	0.99467	0.99467
	Polynomial	0.99067	0.99088	0.99067	0.99066
Color + LBP	Linear	0.99733	0.99733	0.99733	0.99733
	RBF	0.99600	0.99601	0.99600	0.99600
	Polynomial	0.99731	0.99731	0.99731	0.99731
Haralick + LBP	Linear	0.99200	0.99203	0.99200	0.99200
	RBF	0.99600	0.99608	0.99600	0.99600
	Polynomial	0.99600	0.99601	0.99600	0.99600
HOG + LBP	Linear	0.98533	0.98600	0.98533	0.98532
	RBF	0.99467	0.99468	0.99467	0.99467
	Polynomial	0.99333	0.99342	0.99333	0.99335
All Features	Linear	0.99333	0.99334	0.99333	0.99333
	RBF	0.99467	0.99470	0.99467	0.99467
	Polynomial	0.96267	0.96653	0.96267	0.96210

Table 2 depicts the results obtained using different feature settings. **In the first experiment setting**, using only RGB mean and standard deviation-based color features, the accuracy for all three kernels is found to be in the range of 0.89067–0.96133. Macro Precision, Macro Recall, and Macro F1-score are also in the same range. The results suggest that it is possible to capture some of the initial differences between dryness classes using only global color information; however, there is significant misclassification due to color overlap between classes. **In the second experimental setting**, using only the Haralick GLCM-based texture feature, the accuracy ranged from 0.91333 to 0.96133. Although there is a slight improvement compared to the color feature, the results are still not completely satisfactory for all classes. That is, this coarse texture-based descriptor can partially capture

the differences between dry, saturated, and clumped surfaces, but some ambiguity remains because it cannot sufficiently capture fine texture patterns. **Similarly, in the third experimental setting**, using only HOG features, the accuracy dropped to only the 0.39–0.40 range, and the macro precision and macro F1-score were below 0.30. This means that the HOG-only configuration behaves almost like random guessing. The HOG configuration used (large cell size and low feature dimension) did not accurately capture the discriminative gradient pattern required in this application; in addition, since the visual difference in dryness level of the loamy soil is mainly based on intensity and micro-texture, only edge orientation-based information proved to be weak here. **In addition, in the fourth experimental setting**, using only LBP-based micro-texture features, the accuracy and macro F1-score for each of the three kernels were found to be between 0.99467 and 0.99733. That is, almost perfect classification was achieved using only LBP. This clearly indicates that the main feature of the visual dryness level lies within the local texture pattern, such as the arrangement of fine grains, cracks, lumps, and pores on the surface, which can be captured very effectively by the LBP descriptor. **Moreover, the fifth experimental setting**, using the color and Haralick textures together, yields an accuracy of 0.97867 for the linear kernel and 0.99467 and 0.99400 for the RBF and polynomial kernels, respectively. The corresponding Macro Precision and Macro Recall are also very close to these values. This combination clearly provides better performance than using color or Haralick alone, indicating that coarse texture information combined with global color can distinguish dryness levels more reliably. **In the sixth experimental setting**, the color and LBP feature set provided the highest and most stable performance among all configurations. The accuracy ranged from 0.99600 to 0.99733, and the Macro F1-score was around 0.997 for all three kernels. This demonstrates that combining the powerful micro-texture descriptor LBP with global RGB color information allows for almost complete separation of different dryness classes. **The seventh experimental setting** represents the combination of Haralick and LBP feature sets. The Haralick and LBP combination has an accuracy of 0.99200–0.99600 and a macro F1-score of around 0.992–0.996. Although slightly lower than Color and LBP, this configuration also demonstrated high-quality and stable performance. The Haralick-based coarse texture information complements the micro-texture feature of LBP. **The feature set of HOG and LBP** was found to be in the range of 0.98533–0.99333. This is a dramatic improvement over the HOG-only results, which show that the model is able to achieve performance close to 0.99 after adding LBP. In this combination, LBP plays the main discriminative role; HOG is only adding limited additional information. **Finally, in the last setting using all features together**, the accuracy for linear and RBF kernels is 0.99333 and 0.99467, respectively, and the macro F1-score is also similar. However, the accuracy for the polynomial kernel is relatively low (0.96267), which indicates an increase in overfitting or numerical instability due to the combined effect of the high-dimensional feature space and complex kernel function. Importantly, the All_Features configuration provides only a small additional gain compared to Color+LBP or Haralick+LBP; in many cases, there is no significant difference. This suggests that the LBP-centric features contain most of the discriminative information, and the additional feature groups provide only marginal improvements.

The best SVM kernel selection: In Figure 4 compares the performance of three types of SVM kernels (linear, RBF, and polynomial) using the Color+LBP and Haralick+LBP feature sets. The precision, accuracy, recall, and F1-scores for the configurations are almost equal and lie in the range of 0.992–0.97, indicating a very high and balanced classification ability of the model. For the (Color + LBP) feature set, the linear and polynomial kernels

achieved accuracy and F1-scores of around 0.997, while the RBF kernel provided equally low (≈ 0.996) performance. For many (Haralick+LBP) feature sets, the linear kernel is relatively low (≈ 0.992), but the RBF and polynomial kernels achieve values of around 0.996. The overall picture shows that all metrics associated with color-based feature sets with LBP-based feature sets achieve higher and more stable performance, and in particular, the (color + LBP) feature set ensures the best performance for the SVM model.

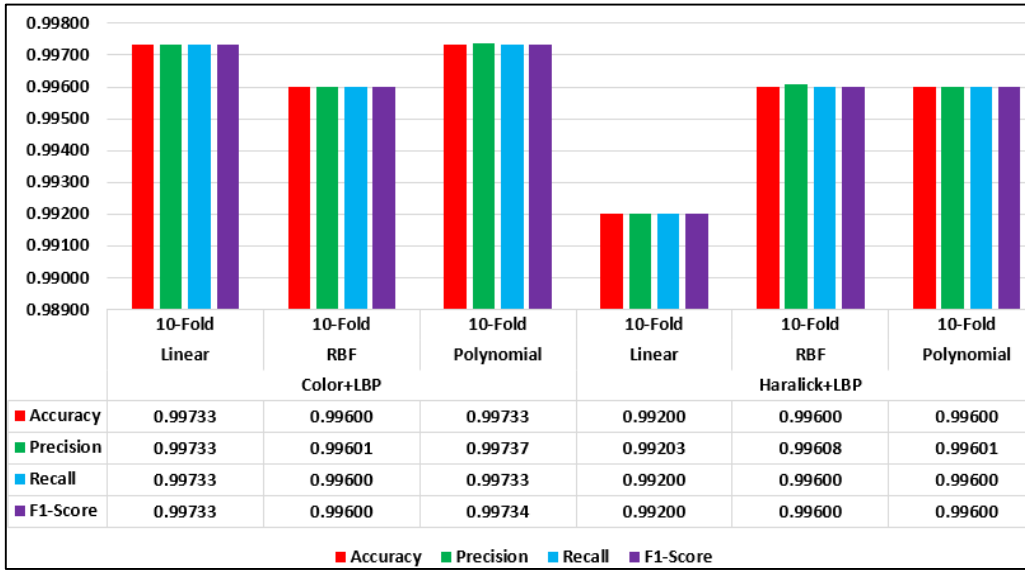


Figure 4: Performance comparison of SVM kernels using Color+LBP and Haralick+LBP feature sets

The Figure 5 shows the comparison of Precision and Recall values of different SVM kernels (Linear, RBF and Polynomial) for the (color + LBP) and Haralick+LBP feature sets.

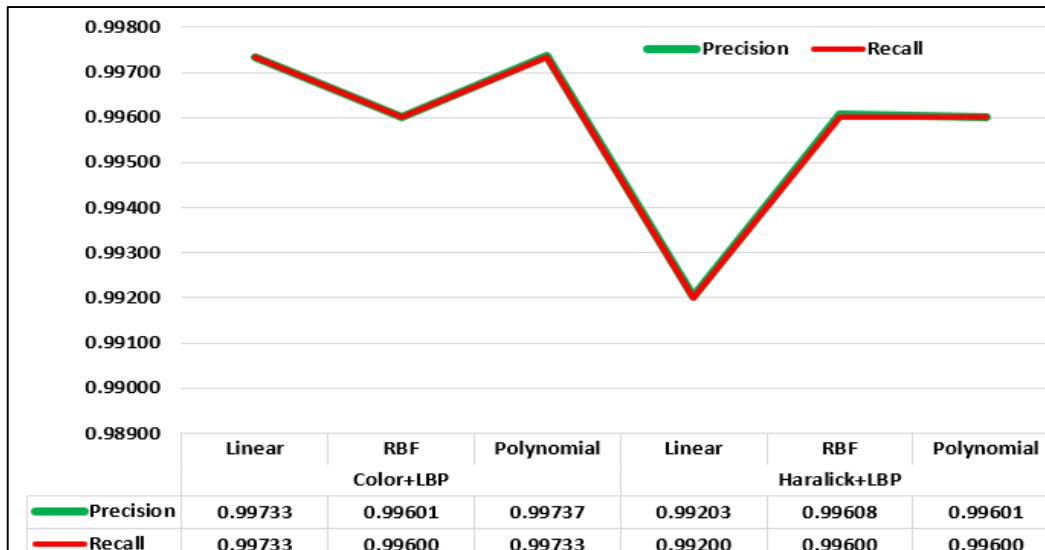


Figure 5: Precision-Recall Curve of SVM kernels with Color+LBP and Haralick+LBP

It can be seen from the graph that Precision and Recall almost completely overlap in all configurations and the

values are between 0.992 and 0.997, indicating a very balanced and reliable classification ability of the models. For the Color + LBP feature set, the Polynomial kernel achieved the highest Precision and Recall around 0.997, while RBF provided slightly lower and Linear provided slightly more stable values. On the other hand, for the (Haralick+LBP) feature set, the Precision and Recall of the Linear kernel are relatively lower (≈ 0.992), while RBF and Polynomial kernels are again around 0.996. Overall, the figure demonstrates that the combination of the selected feature set and SVM kernel achieves almost equal Precision and Recall with very few false positives and false negatives, making the proposed system reliable enough for practical use. The histogram analysis illustrated in Figure 6 indicates that the distribution of intensity across the RGB channels varies with changes in the moisture content of Loamy soil. In a dry state, the soil exhibits relatively high and uniform intensity, leading to a light and bright reflection. Conversely, as the moisture content increases, the intensity values decrease, resulting in a discrete or complex pattern, particularly evident in wet and very wet soils. Thus, these variations in the RGB histogram can serve as an effective indicator for predicting soil moisture content.

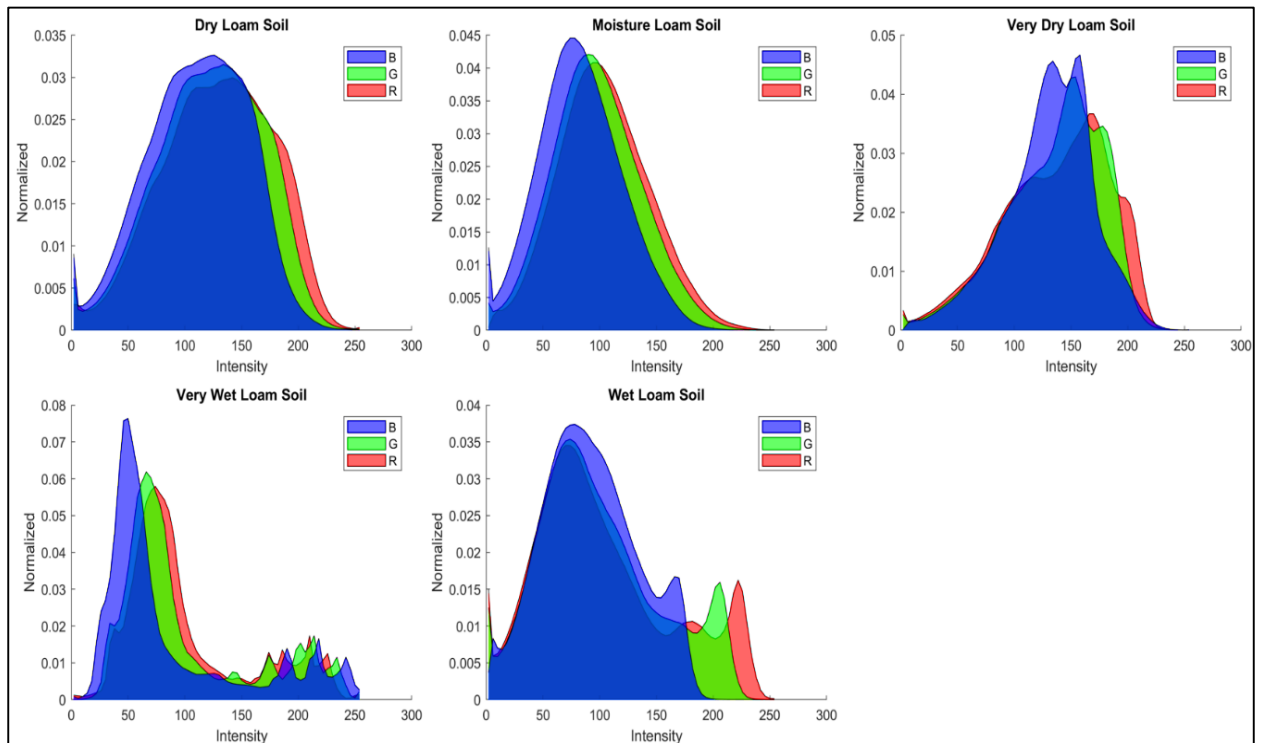


Figure 6: Comparative Analysis of RGB Intensity Distributions of Different Loamy Soils

Comparison with recent study: Table 3 illustrates a comparative analysis of our proposed method with recent studies, where the performance of the models is evaluated considering various performance indicators. The table 3 demonstrate that while the CNN-based method used in Shuaeb and his colleagues [1] study represent a high level of accuracy, our proposed SVM-based model achieves better results in all metrics—accuracy, precision, recall, and F1-score. In particular, while the maximum performance of the CNN method is around 0.978, our proposed SVM method shows a significant improvement by achieving a score of around 0.9991.

Table 3: Demonstrates a comparative analysis between recent studies and the proposed method for soil dryness prediction

Comparison with Recent Study	Used Method	Accuracy	Precision	Recall	F1-score
Shuaeb and his colleagues [1]	CNN	0.9781	0.9778	0.9778	0.9778
Proposed Method	SVM	0.99733	0.99733	0.99733	0.99733

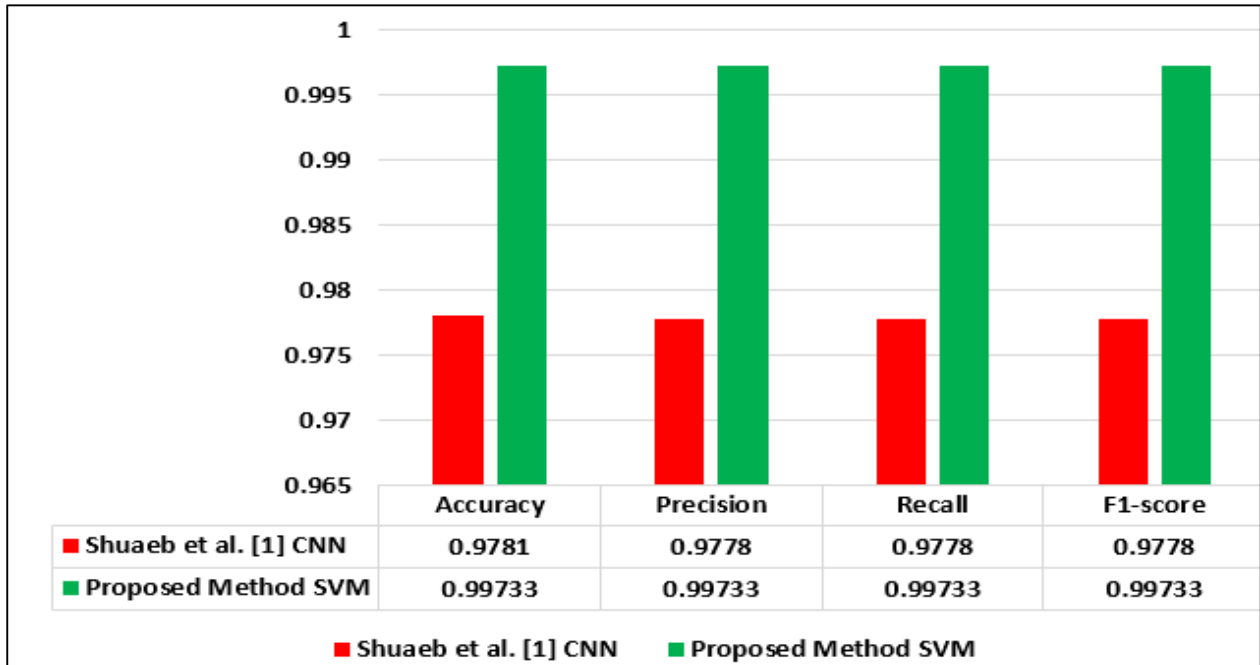


Figure 7: Four Standard Performance Metrics Comparison: CNN vs. Proposed SVM

As a result, the table 3 clearly shows that the proposed model is more reliable and effective than the existing methods in soil dryness prediction. The Figure 7 depicts a comparison of the performance of the CNN model used in recent studies and our proposed SVM model.

In each of the four standard evaluation matrices namely Accuracy, Precision, Recall, and F1-score—the SVM model (green bars) clearly outperformed the CNN (red bars). While the CNN achieved values close to 0.978 in each case, the SVM performed close to 0.997. As a result, the graph clearly represents that the SVM model is capable of providing more accurate, stable, and effective results in Loamy soil dryness prediction.

4. Discussion

The proposed image-based multiclass classification method in this study has demonstrated very high accuracy in determining the dryness level of loamy soil, where an SVM classifier based on color, HOG, LBP, and Haralick-based hybrid feature vectors is used. The experimental results show that the five classes (Very Dry, Dry, Moist, Wet, and Very Wet) become almost linearly separable when appropriate feature fusion and normalization

techniques are applied; thus, even the relatively simple Linear SVM is able to achieve almost perfect classification ability. Statistical analysis shows that the LBP-centric hybrid feature set performs significantly better than the single-color or single-texture features. This means that the dryness of loamy soil is best expressed through the subtle changes in local micro-texture and brightness, which the LBP descriptor can capture very effectively; the color, Haralick, or HOG only helps it. On the other hand, using all the features together leads to a slight performance drop and possible overfitting in some configurations (especially high-dimensional feature + polynomial kernel). This suggests that feature selection and dimension control are important design parameters in this type of classification problem. Although some previous studies have used CNN-based models, a properly tuned SVM-based model on a limited dataset can provide higher accuracy at a relatively low computational cost—as is evident in Table 3. However, since this dataset is mainly collected from a specific geographical region, specific soil, and controlled lighting conditions, additional tests are needed to verify the generalization of the model to different areas, different soil types, and changing lighting in the real field. In the future, introducing larger datasets, different soil types, and continuous moisture estimation will broaden the applicability of the proposed method.

5. Potential Impact on Agriculture in Bangladesh

The proposed image-based soil moisture prediction system can serve as a low-cost and easily accessible tool in the agricultural sector in Bangladesh. By analyzing soil images taken with a simple smartphone or camera, farmers can get an instant idea of soil moisture levels without lab-based testing. Through this, irrigation timing, irrigation volume, and frequency will become more scientific and data-driven, which will help reduce the wastage of water, electricity, and fuel. Soil moisture is closely related to the effectiveness of fertilizers, pesticides, and other inputs. Applying fertilizers and pesticides at the right time at the right moisture level will reduce input wastage, and environmental pollution will also be reduced relatively. At the same time, integration with such image-based moisture mapping and remote sensing platforms in large agricultural areas will provide important information support for drought risk assessment, irrigation project planning, and climate-smart agriculture development. The use of this technology is especially relevant in river basins, loamy soil-dominated areas, and drought-sensitive areas. If the proposed model can be integrated with a mobile app or web-based agricultural advisory platform, extension services, or smart farm management systems, it will be possible to easily expand digital agricultural services to the rural level. In the long run, such low-cost, scalable, and non-invasive solutions can have a significant positive impact on the country's food security, water management, and increasing farmer income.

6. Conclusion

This study demonstrates a low-cost, non-invasive multi-class classification framework for identifying five levels of dryness of loamy soil (Very Dry, Dry, Moist, Wet, and Very Wet) through smartphone-based image analysis. Using a hybrid feature vector and SVM classifier composed of color, Haralick, HOG, and LBP, an accuracy and macro F1-score of about 0.997 were achieved in the best configuration. The experimental results show that the LBP-centric feature set, especially Color+LBP or Haralick+LBP, and the SVM model with a linear or RBF kernel provide a very effective and stable solution for determining the dryness of loamy soil. The major

strengths of the proposed method are its low cost, easy implementation, and applicability to ordinary cameras or smartphones, through which it is possible to make field-level decision-making, including determining the timing and amount of irrigation, more information-based. However, the dataset used was limited to a specific region and a controlled environment. If tested in the future on larger datasets in different geographical areas, different soil types, and changing light environments, compared with deep learning-based models, and implemented as a lightweight mobile/web app, this system could become an effective and widely used smart decision-support tool for farmers.

Acknowledgments

This research was supported by a research grant provided by Dr. Mahbubun Nahar, Jatiya Kabi Kazi Nazrul Islam University, Bangladesh. The authors are deeply grateful for her generous support.

7. Conflicts of Interest Statement

The authors declare no conflict of interest.

8. Data availability Statement

The data that support the findings of this study are openly available in Kaggle at <https://www.kaggle.com/datasets/shuaebnixon/Loamyy-soil-dryness-image>.

Reference

- [1] S. M. A. Al Shuaeb, Md. R. Hassan, and M. Uddin, “Soil Wetness Classification in Agriculture Using Machine Learning Models,” *Asian Journal of Soil Science and Plant Nutrition*, vol. 10, no. 4, pp. 803–815, Dec. 2024, doi: 10.9734/ajsspn/2024/v10i4451.
- [2] Y. Ren, F. Ling, and Y. Wang, “Research on provincial-level soil moisture prediction based on extreme gradient boosting model,” *Agriculture*, vol. 13, no. 5, p. 927, 2023.
- [3] D. Acharjee, N. Mallik, D. Das, M. Aktar, and P. Majumdar, “Crop Yield and Soil Moisture Prediction Using Machine Learning Algorithms,” *Machine Learning Applications: From Computer Vision to Robotics*, pp. 183–194, 2023.
- [4] R. Stiglitz, E. Mikhailova, C. Post, M. Schlautman, and J. Sharp, “Using an inexpensive color sensor for rapid assessment of soil organic carbon,” *Geoderma*, vol. 286, pp. 98–103, 2017.
- [5] H. Kim, M. H. Cosh, R. Bindlish, and V. Lakshmi, “Field evaluation of portable soil water content sensors in a sandy loam,” *Vadose Zone Journal*, vol. 19, no. 1, p. e20033, 2020.
- [6] S. Ibáñez-Asensio, A. Marques-Mateu, H. Moreno-Ramón, and S. Balasch, “Statistical relationships between soil colour and soil attributes in semiarid areas,” *Biosyst Eng*, vol. 116,

no. 2, pp. 120–129, 2013.

- [7] S.-O. Chung, K.-H. Cho, J.-W. Kong, K. A. Sudduth, and K.-Y. Jung, “Soil texture classification algorithm using RGB characteristics of soil images,” *IFAC Proceedings Volumes*, vol. 43, no. 26, pp. 34–38, 2010.
- [8] W. Jiao, J. Wang, Y. He, X. Xi, and X. Chen, “Detecting soil moisture levels using battery-free Wi-Fi tag,” *arXiv preprint arXiv:2202.03275*, 2022.
- [9] Y. Liu, H. Wang, H. Zhang, and K. Liber, “A comprehensive support vector machine-based classification model for soil quality assessment,” *Soil Tillage Res*, vol. 155, pp. 19–26, 2016.
- [10] M. Uddin and M. R. Hassan, “A novel feature based algorithm for soil type classification,” *Complex and Intelligent Systems*, vol. 8, no. 4, pp. 3377–3393, Aug. 2022, doi: 10.1007/s40747-022-00682-0.
- [11] R. Zhu and Y. Wang, “Application of Improved Median Filter on Image Processing,” *J. Comput.*, vol. 7, no. 4, pp. 838–841, 2012.
- [12] T. Sun and Y. Neuvo, “Detail-preserving median based filters in image processing,” *Pattern Recognit Lett*, vol. 15, no. 4, pp. 341–347, 1994.
- [13] M. Kaur, J. Kaur, and J. Kaur, “Survey of contrast enhancement techniques based on histogram equalization,” *International Journal of Advanced Computer Science and Applications*, vol. 2, no. 7, 2011.
- [14] C. Zuo, Q. Chen, and X. Sui, “Range limited bi-histogram equalization for image contrast enhancement,” *Optik (Stuttg)*, vol. 124, no. 5, pp. 425–431, 2013.
- [15] S. M. A. Al Shuaeb, A. Hossen, M. A. H. Dinar, and U. K. Roy, “Analyzing Different Architectures of Convolutional Neural Networks for Tomato Grading System,” *Asian Journal of Research in Computer Science*, vol. 17, no. 12, pp. 137–147, Dec. 2024, doi: 10.9734/ajrcos/2024/v17i12534.
- [16] A. Yadav *et al.*, “Handcrafted Feature and Deep Features Based Image Classification Using Machine Learning Models,” *National Academy Science Letters*, 2025, doi: 10.1007/s40009-025-01616-3.
- [17] A. Lopez-Alanis, H. De-la-Torre-Gutierrez, and A. Hernández-Aguirre, “A thresholdless wildfire pixel detection employing color contrast features,” *Applied Intelligence*, vol. 55, no. 17, Nov. 2025, doi: 10.1007/s10489-025-07004-0.
- [18] M. K. Singh, “DWT and LBP hybrid feature based deep learning technique for image splicing

forgery detection,” *Soft comput*, vol. 28, no. 20, pp. 12207–12215, Oct. 2024, doi: 10.1007/s00500-024-09919-1.

[19] R. Pal, S. Kumar, and M. K. Singh, “Topological data analysis and image visibility graph for texture classification,” *International Journal of System Assurance Engineering and Management*, 2024, doi: 10.1007/s13198-024-02272-4.

[20] S. Suthaharan, “Support vector machine,” in *Machine learning models and algorithms for big data classification: thinking with examples for effective learning*, Springer, 2016, pp. 207–235.

[21] L. H. Thai, T. S. Hai, and N. T. Thuy, “Image classification using support vector machine and artificial neural network,” *International Journal of Information Technology and Computer Science*, vol. 4, no. 5, pp. 32–38, 2012.

[22] F. Bovolo, L. Bruzzone, and L. Carlin, “A novel technique for subpixel image classification based on support vector machine,” *IEEE Transactions on Image Processing*, vol. 19, no. 11, pp. 2983–2999, 2010.

[23] S. S. T. Gontumukkala, Y. S. V. Godavarthi, B. R. R. T. Gonugunta, R. Subramani, and K. Murali, “Analysis of image classification using SVM,” in *2021 12th International Conference on Computing Communication and Networking Technologies (ICCCNT)*, 2021, pp. 1–6.

[24] S. Y. Chaganti, I. Nanda, K. R. Pandi, T. G. Prudhvith, and N. Kumar, “Image Classification using SVM and CNN,” in *2020 International conference on computer science, engineering and applications (ICCSEA)*, 2020, pp. 1–5.

[25] P. Sridhar and P. Angamuthu, “Enhancing image based classification for crop disease detection using a multiclass SVM approach with kernel comparison,” *Sci Rep*, vol. 15, no. 1, Dec. 2025, doi: 10.1038/s41598-025-23568-w.

[26] S. R. Kumar, M. A. Srinivasu, A. Vamsidhar, and B. D. Reddy, “Enhancing rice leaf disease classification accuracy with svm kernels using image embedding techniques for feature extraction: a comprehensive analysis,” *Multimed Tools Appl*, Oct. 2025, doi: 10.1007/s11042-025-20831-0.

[27] O. Abda and H. Naimi, “Advanced Brain Tumor MR Image Classification Using a Combination Undecimated Wavelet Transform, EfficientNet-B0 and PCA via Multi-SVM Analysis,” *Iranian Journal of Science and Technology - Transactions of Electrical Engineering*, vol. 49, no. 2, pp. 601–613, Jun. 2025, doi: 10.1007/s40998-025-00801-w.

[28] B. Hossain, U. K. Roy, Shamsunnaher, Md. S. A. A. Kawser, and S. M. A. Al Shuaeb, “Image-based Pest Identification Using Support Vector Machine for Agricultural Crop Protection,”

Asian J Res Crop Sci, vol. 10, no. 3, pp. 13–22, Jun. 2025, doi: 10.9734/ajrcs/2025/v10i3368.

[29] H. Dalianis, “Evaluation metrics and evaluation,” in *Clinical Text Mining: secondary use of electronic patient records*, Springer, 2018, pp. 45–53.

[30] Ž. Vujović and others, “Classification model evaluation metrics,” *International Journal of Advanced Computer Science and Applications*, vol. 12, no. 6, pp. 599–606, 2021.

[31] F. Daghistani and H. Abuel-Naga, “Evaluating the influence of sand particle morphology on shear strength: A comparison of experimental and machine learning approaches,” *Applied Sciences*, vol. 13, no. 14, p. 8160, 2023.